arXiv:1410.5571v1 [physics.optics] 21 Oct 2014

# Broadband, stable and highly coherent supercontinuum generation at telecommunication wavelengths in an hydrogenated amorphous silicon waveguide

**F. Leo[1,2], J. Safioui[3], B. Kuyken[1,2], G. Roelkens[1,2] and S.-P. Gorza[3]**

[1] *Photonics Research Group, Department of Information Technology, Ghent University-IMEC, Ghent B-9000, Belgium*

[2] *Center for nano- and biophotonics (NB-photonics), Ghent University, Belgium*

[3] *Service OPERA-photonique, Université libre de Bruxelles (ULB), 50 Avenue F. D. Roosevelt, CP194/5 B-1050 Bruxelles, Belgium.*

*sgorza@ulb.ac.be*

**Abstract:**
Hydrogenated amorphous silicon (a:Si-H) has recently been recognized as a highly nonlinear CMOS compatible photonic platform. We experimentally demonstrate the generation of a supercontinuum (SC) spanning over 500 nm in a-Si:H photonic wire waveguide at telecommunication wavelengths using femtosecond input pulse with energy lower than 5 pJ. Numerical modeling of pulse propagation in the waveguide, based on the experimentally characterized dispersion profile, shows that the supercontinuum is the result of soliton fission and dispersive wave generation. It is demonstrated that the SC is highly coherent and that the waveguides do not suffer from material degradation under femtosecond pulse illumination. Finally, a direct comparison of SC generation in c-Si and a-Si:H waveguides confirms the higher performances of a-Si:H over c-Si for broadband low power SC generation at telecommunication wavelengths.

© 2014 Optical Society of America

**OCIS codes:** (320.6629) Supercontinuum generation; (130.4310) Integrated optics, Nonlinear; (190.5530) Nonlinear optics, Pulse propagation and temporal solitons

## References and links

1. R. R. Alfano and S. L. Shapiro, "Observation of self- phase modulation and small-scale filaments in crystals and glasses," Phys. Rev. Lett. **24,** 592-594 (1970).
2. J. M. Dudley, G. Genty, and S. Coen, "Supercontinuum generation in photonic crystal fiber," Rev. Mod. Phys. **36,** 1135-1184 (2006).
3. M. R. Lamont, B. Luther-Davies, D.-Y. Choi, S. Madden, and B. J. Eggleton, "Supercontinuum generation in dispersion engineered highly nonlinear($\gamma$ = 10 /W/m) $As_2S_3$ chalcogenide planar waveguide," Opt. Express **16,** 14938 (2008).
4. R. Halir,Y. Okawachi, J.S. Levy, M.A. Foster, M. Lipson, and A. L. Gaeta, "Ultrabroadband supercontinuum generation in a CMOS-compatible platform," Opt. Lett. **37,** 1685 (2012).
5. J. Safioui, F. Leo, B. Kuyken, S-P Gorza, S K Selvaraja, R Baets, Ph. Emplit, G Roelkens, and S Massar, "Supercontinuum generation in hydrogenated amorphous silicon waveguides at telecommunication wavelengths," Opt. Express **22,** 3089-3097 (2014).

6. I. Hsieh, X. Chen, X. Liu, J. Dadap, N. Panoiu, C. Chou, F. Xia, W. Green, Y. Vlasov, and R. Osgood, "Supercontinuum generation in silicon photonic wires," Opt. Express **15,** 15242-15249 (2007).
7. W. Ding, A. V. Gorbach, W. J. Wadswarth, J. C. Knight, D. V. Skryabin, M. J. Strain, M. Sorel, and R. M. De La Rue, "Time and frequency domain measurements of solitons in subwavelength silicon waveguides using a cross-correlation technique," Opt. Express **39,** 26625-26630 (2010).
8. F. Leo, S.-P. Gorza, J. Safioui, P. Kockaert, S. Coen, U. Dave, B. Kuyken, and G. Roelkens, "Dispersive wave emission and supercontinuum generation in a silicon wire waveguide pumped around the 1550 nm telecommunication wavelength," Opt. Lett. **39,** 3623 (2014).
9. A. Ishizawa1, T. Goto, H. Nishi, N. Matsuda, R. Kou, K. Hitachi, T. Nishikawa, K. Yamada, T. Sogawa, and H. Gotoh, "On-Chip Supercontinuum Generation in a Dispersion- Controlled Silicon-Wire Waveguide," Conference on Laser and Electro-Optics 2014, ATu3P.3, San-Jose (2014).
10. L. Zhang, Q. Lin, Y. Yue, Y. Yan, R. G. Beausoleil, A. Agarwal, L. C. Kimerling, J. Michel, and A. E. Willner, "On-Chip Octave-Spanning Supercontinuum in Nanostructured Silicon Waveguides Using Ultralow Pulse Energy," IEEE J. Selec. Topics Quant. Electron. **18,** 1799-1805 (2012).
11. B. Kuyken, X. Liu, R. M. Osgood Jr., R. Baets, G. Roelkens, and W. M. J. Green, "Mid-infrared to telecom-band supercontinuum generation in highly nonlinear silicon-on-insulator wire waveguides," Opt. Express **19,** 20172 (2011).
12. L. Shen, N. Healy, L. Xu, H. Y. Cheng, T. D. Day, J. H. V. Price, J. V. Badding, and A. C. Peacock, "Four-wave mixing and octave-spanning supercontinuum generation in a small core hydrogenated amorphous silicon fiber pumped in the mid-infrared," Opt. Lett., **39,** 5721-5724 (2014).
13. K. Ikeda, Y. Shen, and Y. Fainman, "Enhanced optical nonlinearity in amorphous silicon and its application to waveguide devices," Opt. Express **15,**, 17761-17771 (2007).
14. K. Narayanan, A. W. Elshaari and S. F. Preble, "Broadband all-optical modulation in hydrogenated-amorphous silicon waveguides," Opt. Express **18,** 9809-9814 (2010).
15. Y. Shoji, T. Ogasawara, T. Kamei, Y. Sakakibara, S. Suda, K. Kintaka, H. Kawashima, M. Okano, T. Hasama, H. Ishikawa, and M. Mori, "Ultrafast nonlinear effects in hydrogenated amorphous silicon wire waveguide," Opt. Express **18,** 5668-5673 (2010).
16. B Kuyken, S Clemmen, S K Selvaraja, W Bogaerts, D Van Thourhout, Ph Emplit, S Massar, G Roelkens, and Roel Baets, "On-chip parametric amplification with 26.5 dB gain at telecommunication wavelengths using CMOS-compatible hydrogenated amorphous silicon waveguides," Opt. Lett. **36,** 552 (2011).
17. K.-Y. Wang and A. C. Foster,"Ultralow power continuous-wave frequency conversion in hydrogenated amorphous silicon waveguides," Opt. Lett. **37,** 1331-1333 (2012).
18. P. Mehta, N. Healy, T. D. Day, J. V. Badding, and A. C. Peacock, "Ultrafast wavelength conversion via cross-phase modulation in hydrogenated amorphous silicon optical fibers," Opt. Express **20,** 26110-26116 (2012).
19. S.-P. Gorza, F. Leo, B. Kuyken, S. K. Selvaraja, G. Roelkens, R. Baets, Ph. Emplit, S. Massar and J. Safioui, "Supercontinuum Generation in Hydrogenated Amorphous Silicon Waveguides in the Femtosecond Regime," Conference on Laser and Electro-Optics 2014, FW1D.7, San-Jose (2014).
20. P. A. Merritt, R. P. Tatam, and D. A. Jackson, "Interferometric chromatic dispersion measurements on short lengths of monomode optical fiber", Journal of Lightwave Technology 7, 703 (1989).
21. F. Leo, U. Dave, S. Keyvaninia, B. Kuyken, and G. Roelkens, "Measurement and tuning of the chromatic dispersion of a silicon photonic wire around the half band gap spectral region," Opt. Lett. 39, 711 (2014).
22. C. Iaconis and I. A. Walmsley, "Self-Referencing Spectral Interferometry for Measuring Ultrashort Optical Pulse," IEEE J. Quant. Electronics, **35,** 501-509 (1999).
23. N. Akhmediev and M. Karlsson, "Cherenkov radiation emitted by solitons in optical fibers,"Phys. Rev. A **51,** 2602 (1995).
24. N. Maley, D. Beerman, and J.S. Lannin, "Dynamics of tetrahedral networks: Amorphous Si and Ge," Phys. Rev. B **38,** 10611 (1988).
25. P. Mehta, N. Healy, N. F. Baril, P. J. A. Sazio, J. V. Badding, and A. C. Peacock," Nonlinear transmission properties of hydrogenated amorphous silicon core optical fibers," Opt. Express **18,** 16826-16831 (2010).
26. J. J. Wathen, V. R. Pagán, R. J. Suess, K.Y. Wang, A. C. Foster, and T. E. Murphy, "Non-instantaneous optical nonlinearity of an a-Si:H nanowire waveguide," Optics Express **22,** 22730 (2014).
27. Y. Silberberg, "Solitons and two-photon absorption," Opt. Lett. **15,** 1005 (1990).
28. F. Leo, S-P Gorza, S. Coen, B. Kuyken, and G. Roelkens, "Coherent Telecommunication Band Supercontinuum Generation in a Silicon Photonic Wire," arXiv:1410.4390.
29. M. Bellini and T. W. Hänsch, "Phase-locked white-light continuum pulses: toward a universal optical frequency-comb synthesizer," Opt. Lett. **25,** 1049-1051 (2000).
30. F. Lu and W. H. Knox, "Generation of a broadband continuum with high spectral coherence in tapered single-mode optical fibers," Opt. Express **12,** 347-353 (2004).
31. D. L. Staebler and C. R. Wronski, "Reversible conductivity changes in discharge-produced amorphous Si," Appl. Phys. Lett. **31,** 292-294 (1977).
32. M. Stutzmann, W. B. Jackson, and C. C. Tsai, "Light-induced metastable defects in hydrogenated amorphous silicon: A systematic study," Phys. Rev. B **32,** 23-47 (1985).

33. H. Fritzsche, "Development in understanding and controlling the Staebler-Wronski effect in a-Si:H," Annu. Rev. Mater. Res. **31,** 47-79 (2001).
34. K. Morigaki, and H. Hikita, "Modeling of light-induced defect creation in hydrogenated amorphous silicon," Phys. Rev. B **76,** 085201 (2007).
35. C. Grillet, L. Carletti, C. Monat, P. Grosse, B. Ben Bakir, S. Menezo, J. M. Fedeli, and D. J. Moss, "Amorphous silicon nanowires combining high nonlinearity, FOM and optical stability," Opt. Express **20,** 22609-22615 (2012).
36. H. K. Tsang and Y. Liu, "Nonlinear optical properties of silicon waveguides," Semicond. Sci. Technol. **23,** 064007 (2008).
37. K. Narayanan and S. F. Preble, "Optical nonlinearities in hydrogenated amorphous silicon waveguides," Opt. Express **18,** 8998-9005 (2010).
38. S. Suda, K. Tanizawa, Y. Sakakibara, T. Kamei, K. Nakanishi, E. Itoga, T. Ogasawara, R. Takei, H. Kawashima, S. Namiki, M. Mori, T. Hasama, and H. Ishikawa, "Pattern- effect-free all-optical wavelength conversion using a hydrogenated amorphous silicon waveguide with ultra-fast carrier decay," Opt. Lett. **37,** 1382-1384 (2012).
39. N. Vukovic, N. Healy, F. H. Suhailin, P. Mehta, T. D. Day, J. V. Badding, and A. C. Peacock , "Ultrafast optical control using the Kerr nonlinearity in hydrogenated amorphous silicon microcylindrical resonators," Sci. Report **3,** 02885 (2013).
40. B. Kuyken, H. Ji, S. Clemmen, S. K. Selvaraja, H. Hu, M. Pu, M. Galili, P. Jeppesen, G. Morthier, S. Massar, L. K. Oxenløwe, G. Roelkens, and R. Baets, "Nonlinear properties of and nonlinear processing in hydrogenated amorphous silicon waveguides," Opt. Express **20,** B146-B153 (2011).
41. A. Demircan, Sh. Amiranashvili,and G. Steinmeyer, "Controlling light by light with an optical event horizon," Phys. Rev. Lett. **106,** 163901 (2011).
42. A. Choudhary, and F. König, "Efficient frequency shifting of dispersive waves at solitons," Opt. Express **20,** 5538-5546 (2012).

## 1. Introduction

Since its first discovery in the early seventies by Alfano and Shapiro [1], the phenomenon of supercontinuum generation (SCG) has been thoroughly studied, particularly since the advent of photonic crystal fibers (PCFs). This fascinating nonlinear process gives rise in the extreme case to octave-spanning spectra and found numerous applications in frequency metrology, spectroscopy, optical communications, or medical imaging [2]. PCF-based supercontinua are nowadays routinely generated in laboratories and SC-sources are commercially available. Recently, the generation of SC in integrated photonics has attracted a lot of attention for its potential for high-volume, low-cost and low power consumption, integrated broadband or few-cycle pulse sources. On-chip supercontinuum generation at wavelengths in the C band of telecommunications has been reported in chalcogenide [3], silicon nitride [4], amorphous silicon [5] and silicon photonic wires [6, 7, 8]. The generation of broad SC spectra in silicon chips is challenging near 1550 nm because two-photon absorption and subsequent free-carriers effects limit the spectral broadening [8]. To overcome this problem, it has been shown that resorting to short pulses ($< 100$ fs) [9] or nanoscale slot waveguides [10] improve the SC bandwidth. An alternative is to seed the SC in the mid-IR where lower nonlinear losses are experienced because the pump photon energy is below the mid bandgap of crystalline silicon [11]. Note that an octave-spanning SC, seeded in the mid-IR, has recently been reported in a-Si:H [12].

Few years ago, hydrogenated amorphous silicon (a-Si:H) has been identified as a very promising material for nonlinear optics at telecommunication wavelengths, either in photonic chips [13, 14, 15, 16, 17] or in optical fibers [18]. As crystalline silicon (c-Si) waveguides, a-Si:H photonic wires can be fabricated with CMOS compatible processes on silicon-on-insulator. However it has the advantage over c-Si of being characterized by a higher nonlinear refractive index and a lower nonlinear absorption coefficient resulting from a larger bandgap energy. Thanks to these favorable properties, the generation of a broad supercontinuum, seeded by picosecond pulses, in a-Si:H waveguides with low anomalous dispersion at 1550 nm has been demonstrated [5]. In this latter work, the initial spectral broadening is the result of spontaneous generation of new frequencies from noise. The generated SC are thus expected to be

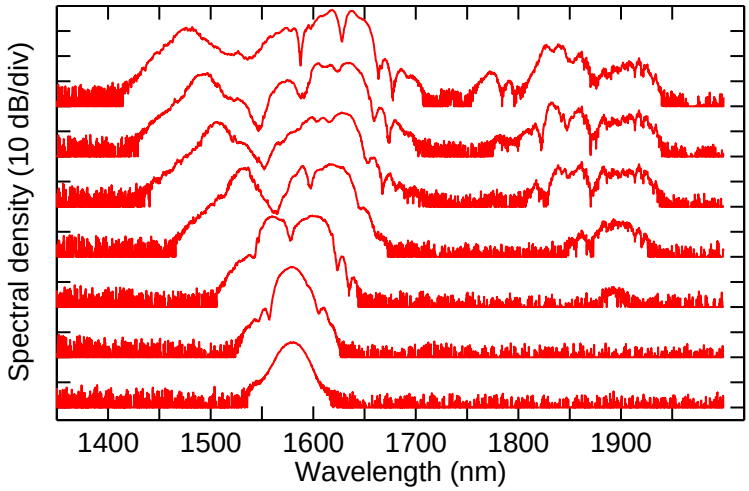


Fig. 1. Spectra recorded at the output of a 1-cm-long a:Si-H waveguide for an input on-chip peak power of 0.03 W, 1.2 W, 2.3 W, 4.6 W, 6.9 W, 9.8 W and 13 W (bottom to top). The curves are shifted by 20 dB for clarity.

incoherent with large amplitude and phase fluctuations from shot-to-shot. In this work, we study the properties of supercontinua seeded by shorter pulses ($<$ 200 fs). In this regime, the initial spectral broadening is expected to be dominated by self-phase modulation [2] and therefore a highly coherent SC should be generated.

## 2. Supercontinuum generation

In our experiments, we consider 1-cm-long, 220-nm-thick and 500-nm-wide hydrogenated amorphous silicon (a:Si-H) photonic wire waveguides. The a-Si:H film was deposited using a low temperature Plasma Enhanced Chemical Vapor Deposition (PECVD) process on top of a 1950 nm thick layer of high-density plasma oxide on a silicon substrate [16]. The input pump was the idler output of an OPO laser pumped by a Ti:Sapphire laser (Spectra Physics OPAL and Tsunami, respectively), which delivers 180 fs pulses at 82 MHz repetition rate. The horizontally-polarized laser output was coupled into the waveguide by means of a $\times$60 microscope objective (NA = 0.65) to excite the quasi-TE mode of the waveguide. At the output, the light was collected by a lensed fiber (NA = 0.4) and sent either into an optical spectrum analyzer or to an interferometer to measure the coherence of the generated SC. The input and output coupling efficiencies were measured to be -20.8 dB and -9.5 dB respectively.

Typical SC spectra at the waveguide output are reported in Fig.1 for seed pulses at 1575 nm and for an on-chip input power ranging from 0.03 to 13 W. As can be seen, as the input power increases, the pump spectrum broadens by self-phase modulation and, at input powers larger than 2.3 W, the spectrum exhibits features far from the pump wavelength around 1900 nm. At high power, i.e. for a pump energy close to 3 pJ, the spectrum extends from 1450 to 1850 nm at -20 dB. Note that in [19] we have reported larger SC spectra spanning from 1380 nm to 1920 nm at -20 dB, at slightly higher power (18 W) and in a similar but not identical waveguide. Referring to [2], at high power, the SC spectrum is likely the result of self-phase modulation, soliton fission and dispersive wave generation. The measurement of the output power as a function of the input power (not shown) reveals that the nonlinear absorption is not negligible and saturates the available output energy in the supercontinuum.

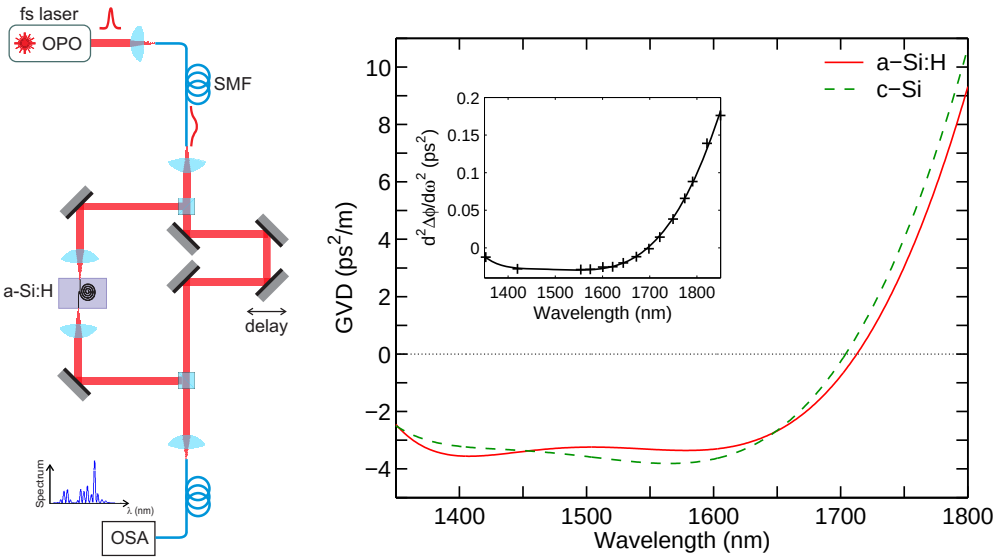


Fig. 2. Left: Experimental setup used to measure the GVD of our nanowires. Right: Measured GVD. The solid red curve shows the fourth-order polynomial fit of $\beta_2(\omega)$ plotted as a function of the wavelength, for our a:Si-H waveguides. The curvature of the phase difference between the reference and the waveguide arms ($d^2\Delta\phi/d\omega^2$) for the 1-cm-long photonic wire is shown in the inset (cross) along with the 4th order polynomial fit of the data (solid line). The green dashed line shows the measured GVD of similar crystalline silicon waveguides (same mask).

## 3. Group velocity dispersion measurement

The dispersion properties of the waveguide play an important role in the SC generation. The spectral characteristics of the SC shown in Fig.1 can thus be fully understood and reproduced in numerical simulations only if the group velocity dispersion (GVD) is known over its whole spectrum. a-Si:H is a material with considerable variation in chemical structure, and different fabrication processes might lead to different material and hence optical properties. In the absence of sufficient data about the refractive index of our a-Si:H film in the wavelength range of interest, we have measured the dispersion properties of the waveguide. The GVD was measured at different wavelengths by resorting to standard spectral interferometric methods [20, 21]. We used an unbalanced free space Mach-Zehnder interferometer in which, in one arm, the light propagates in the waveguide under test (see Fig. 2). The light source was the signal ($\sim 1350$ nm) or the idler ($1550-1750$ nm) output of the OPO laser, or alternatively a SLED light source (1500-1600 nm). In order to avoid any nonlinear effects in the waveguide, the pulses at the output of the OPO were temporally broadened by propagation through SMF fiber. At the output of the interferometer, the spectral fringes between the pulses from the two arms were recorded with an optical spectrum analyzer. Thanks to the nonzero delay between the two pulses, their spectral phase difference ($\Delta\phi(\omega)$) can readily be extracted by numerically filtering the Fourier transform of the interference pattern [22]. The inset in Fig. 2 shows the second order derivative $d^2\Delta\phi/d\omega^2$ as a function of the wavelength, for the 1-cm-long waveguide. Each cross corresponds to one measurement. This data were fitted by a fourth order polynomial curve in the frequency domain. In order to extract the GVD, the measurements were done for 1 and 2 cm-long waveguides. The GVD plotted in Fig. 2 is thus given by $\beta_2(\omega) = [d^2\Delta\phi_{2cm}/d\omega^2 - d^2\Delta\phi_{1cm}/d\omega^2]/1\text{cm}$.

It can be seen that at telecommunication wavelengths, the dispersion is anomalous and is

about -3.3 $ps^2$/m. This value is in agreement with previous results based on the estimation of $\beta_2$ from a four-wave-mixing experiment [16] in similar waveguides. The zero-dispersion wavelength is measured to be about 1710 nm, meaning that part of the SC spectrum reported in Fig.1 is in the normal dispersion regime. This suggests that the spectral broadening is partially the result of the resonant energy transfer from the strong pump pulse propagating in the anomalous GVD regime to a Čerenkov dispersive wave in the normal dispersion regime[23]. The phase-matching condition associated with dispersive wave emission is $\sum_{k\geq 2}\beta_k(\omega_{DW}-\omega_s)^k/k! = \gamma P$, where $\beta_k$ are the dispersion coefficients associated with the Taylor series expansion of the propagation constant around the pump frequency $\omega_s$ and $\omega_{DW}$ is the frequency of the dispersive wave. This condition predicts the dispersive wave to be emitted at $\lambda_{DW} = 1950$ nm in good agreement with the small spectral peak seen in Fig. 1 at 2.3 W peak power. This also confirms the results reported in [5], where SC generation was investigated in the picosecond regime in similar waveguides.

## 4. Numerical simulations

Further insights about the underlying physics of SC generation in the a-Si:H waveguides displayed in Fig. 1 can be gained by numerically simulating the propagation of the optical field. The model considered is the generalized nonlinear Schrödinger equation (GNLSE), where higher order dispersion and self-steepening terms are included:

$$\frac{\partial A(z,t)}{\partial z} = i\sum_{k=2}^{6}\frac{i^k}{k!}\beta_k\frac{\partial^k A(z,t)}{\partial t^k} - \frac{\alpha_0}{2}A(z,t) + i(1+\frac{i}{\omega_0}\frac{\partial}{\partial t})A(z,t)\int_{-\infty}^{\infty}R(t')|A(z,t-t')|^2dt'. \quad (1)$$

In this equation $A(z,t)$ is the slow-varying envelope of the electric field, $R(t) = \gamma\delta(t)$ with $\gamma = (770 + i30)\,W^{-1}m^{-1}$ [16] and the coefficients $\beta_k$ are extracted from the measurements reported in Fig. 2. The linear losses were measured to be 2.65 dB/cm by cutback method.

Raman scattering has been reported both in a-Si and in a-Si:H [24, 25]. However, its weakness prevented us to see evidence of the Raman contribution in previous studies with our a-Si:H photonic wires. The Raman effect was thus neglected in Eq.1. In crystalline silicon, where free-carrier index change (FCI) and free-carrier absorption (FCA) are well known, it has been shown that FCI and FCA do not sgnificantly modify the SC generation in the femtosecond regime [8]. We have thus not considered the FCA and FCI contribution. Finally note that it has recently been reported in [26] that hydrogenated amorphous silicon waveguides might show absorptive and refractive non-instantaneous nonlinearity [13] as well as no instantaneous nonlinear absorption. We have not included these results in our model because these effects are not known for our waveguide and might strongly depend on the fabrication process as suggested by the variety of nonlinear characteristics of a-Si:H waveguides reported in literature (see e.g. [15]).

The measurement of the autocorrelation trace and the spectrum of the input pulses agree well with a Gaussian pulse shape $E = A_0 exp(-[t/T_0]^2)$ with $T_0 = 160$ fs. At a moderate peak power of 2.3 W, i.e. for a soliton number $N = [T_0^2 \mathrm{Re}\{\gamma\}P_0/(2\beta_2)]^{1/2} = 2.6$, the numerical simulation shows that the pump spectrum is broaden by self-phase modulation in the first millimeters of propagation (see Fig. 3(a)). This broadening is accompanied by a temporal compression and is followed by a splitting of the initial high-order soliton in two solitons with almost equal power. The origin of the soliton fission mechanism is attributed to TPA as demonstrated in c-Si waveguide [8], despite the lower TPA coefficient encountered in a-Si:H. Without TPA, numerical simulations reveal that solition fission induced by high-order dispersion leads to two fundamental solitons with unequal pulse width and amplitude, and thus to a strongly asymmetric output spectrum. On the contrary, with the TPA alone the two pulses have the same amplitude and temporal width, resulting in a symmetric spectrum around the carrier frequency, as shown in [27] for weak TPA, and in agreement with the shape of the experimental output

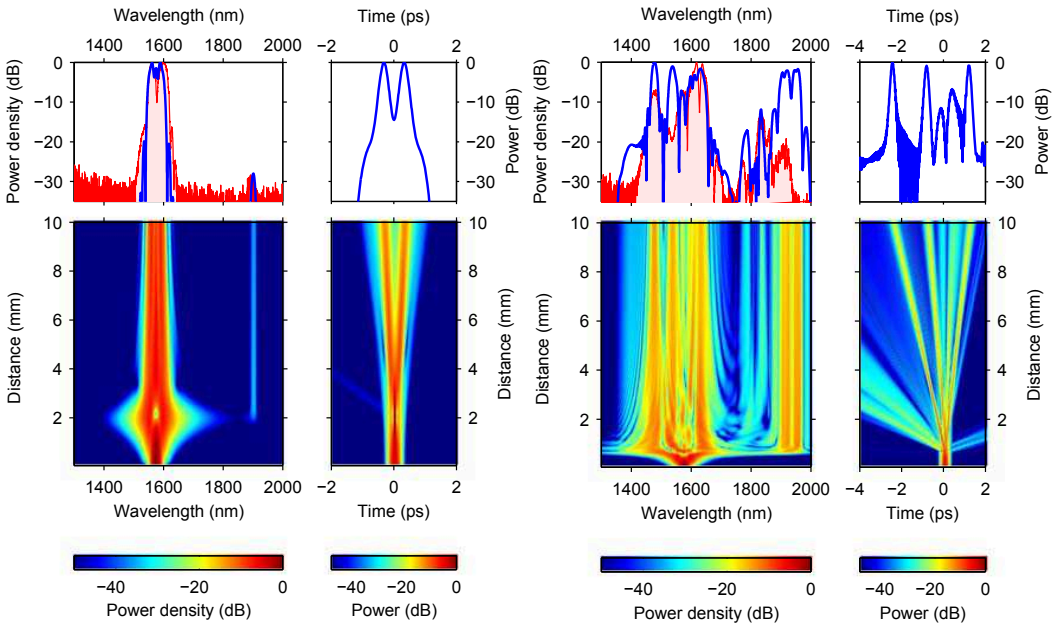


(a) P=2.3W (b) P=13W

Fig. 3. Pseudocolor plots of the simulated spectral and temporal evolution along the propagation for a 2.3 W (left) and 13 W (right) 188 fs Gaussian input pulse (FWHM). Top plots (blue) highlight the waveguide output at z = 10 mm. The red filled curve is the measured output spectrum for comparison (see also in Fig. 1).

spectra. Finally, the small normal GVD peak around 1.9 $\mu$m is related to the emission of a dispersive wave and its position is in excellent agreement with the experiment.

As for SC generation in photonic crystal fibers [2], at higher input peak power (13 W), it can be noticed that the spectral broadening is approximately symmetrical in the initial stage of propagation(see Fig. 3(b)). At about 0.6 mm, the temporal compression is maximum and the simulations show that the input pulse is compressed down to 16 fs, revealing the potential of a-Si:H waveguides for on-chip ultrashort pulse generation. After the compression stage, the spectrum becomes asymmetric with the emergence of a large peak in the normal dispersion regime due to the generation of a strong dispersive wave, and the development of distinct spectral peaks around the pump wavelength. These peaks are related in the temporal domain, with the splitting of the initial pulse into five sub pulses with different temporal duration and peak power. The soliton number at the input is $N = 6.2$, a value close to the number of ejected pulses. This is in contrast with the results reported in c-Si at telecommunication wavelengths where the pulse splitting results in the generation of a small number, largely lower than the initial soliton number, of equal fundamental solitons, because of the large TPA experienced in this latter structure [28].

After 1 cm of propagation, the numerically simulated spectrum qualitatively agrees with the recorded output spectrum. In the anomalous dispersion region ($\lambda < 1720$ nm), the edge of the two spectra near the ZDW agree very well and no evidence of Raman self-frequency shift is visible. This confirms our assumption that Raman effect does not play a significant role in the SC generation. The differences in the spectral features might be attributed to our model, where we only assume instantaneous refractive and absorptive nonlinearities. In the normal dispersion

regime, numerical simulations show an efficient transfer of energy to the dispersive wave up to 25% of the total output energy. In our experiment, the spectral peaks are lower in that region, particularly beyond 1.9 $\mu$m. This might be attributed to a linear loss larger than expected in that wavelength range.

## 5. Coherence

An important characteristic of a supercontinuum is its shot-to-shot stability and, for some applications such as coherent spectroscopy or frequency metrology, a stable and coherent SC over its entire spectral bandwidth is highly desirable. Extensive studies of SC generation in PCF and conventional fibers have shown that the sensitivity of the SC to noise is inherently related to the nature of the spectral broadening processes involved. The coherence property of SC can be viewed as the result of a competition between soliton fission and modulation instability [2]. The spectral coherence of the SC thus depends on dispersion and nonlinear properties of the waveguide but also on the pulse duration and peak power of the seed pulse. It is thus expected the SC reported in the picosecond regime in a:Si-H waveguides in [5] to show poor coherence and the one displayed in Fig. 1 to be coherent, though the waveguides are similar in both experiments. Indeed, the broadening mechanism in the latter case is dominated by soliton fission with a relatively low input soliton number ($N < 10$), making the SC less sensitive to pump laser shot noise.

The coherence properties of the SC generated in the a:Si-H photonic wires with $< 200$ fs input pulses have been studied through the degree of first-order coherence $|\gamma_{12}^{(1)}(\lambda,t,t+\tau)|$, similarly to our work carried out in c-Si waveguides [28] . This was performed by sending the SC collected at the output of the a:Si-H waveguide into an unbalanced Michelson interferometer where the delay $\tau$ between the two arms almost matches the pulse delay between two successive laser pulses [29] (see [28] for further details on the experimental setup). The spectral interference pattern resulting from two successive independent SCs was thus measured by a spectrum analyzer (see insets in Fig. 4).

The degree of first-order coherence can readily be extracted from the fringe visibility $V = (I_{\max} - I_{\min})/(I_{\max} + I_{\min})$ where $I_{\max,\min}$ are the maximum and minimum values of the fringe pattern: $V = 2|\gamma_{12}^{(1)}|[I_1 I_2]^{1/2}/(I_1 + I_2))$ where $I_{1,2}$ are the intensities in each arm. The experiment was performed for a SC seeded at a wavelength of 1620 nm. This wavelength, closer to the zero-dispersion wavelength (ZDW), allows to generate an almost gap-free SC from 1450 nm to 1900 nm, together with strong signals in the normal dispersion regime. Several interference patterns were recorded, each slightly different due to a small drift of the fringes between two scans. The visibility at a given wavelength was measured by looking at the maximum and the minimum values of the fringes at that wavelength among our data set. The spectral resolution was 1 nm, to avoid degradation of the visibility though ensuring a sufficiently high signal-to-noise ratio, given the weakness of the signal collected at the output of the interferometer.

As can be seen in Fig. 4, the visibility is better than 0.9 almost everywhere in the SC spectrum. The measured values constitute a lower limit for $|\gamma_{12}^{(1)}|$ because of the intensity difference between the two arms in some portions of the spectrum, and the noise floor of the OSA which prevents us to properly measure $I_{\min}$. This high visibility shows that the generated SC is highly coherent and stable across its whole spectral bandwidth as for SC in c-Si [28]. This contrasts with the coherence measured in PCF with input pulses in the range 100-200 fs in the anomalous dispersion region [30].

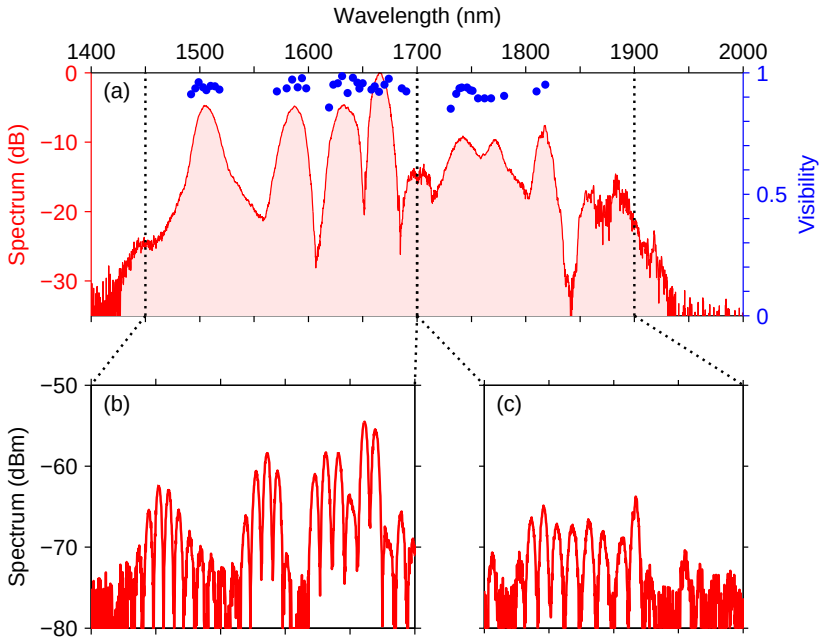


Fig. 4. Experimental results: (a) Normalized spectrum at the output of the waveguide. (b) Spectrum at the output of the interferometer when aligned to maximize the transmission in the 1450-1750 nm spectral region. (c) Same as (b) but for the 1650-1950 nm spectral region. The measured deep fringes indicate strong phase locking accross the supercontinuum. Note that due to experimental constraints, the amplitudes in the two arms are not equal on the whole spectral windows. The fringe visibility thus gives the minimum value of the first order coherence.

## 6. Material stability

Hydrogenated amorphous silicon is a commonly used material for large-area electronics and optoelectronics. However this material suffers from degradation of its optoelectronic properties under illumination, known as the Staebler-Wronski effect (SWE) [31]. This effect is associated with light-induced creation of dangling bonds originating from breaking of weak Si-Si bonds adjacent to a Si-H bond under illumination [32, 33, 34]. Previous experiments on similar waveguides as in this work [5, 16], have reported a degradation of their nonlinear properties under illumination at telecommunication wavelengths, presumably from two-photon absorption induced SWE. However, unlike c-Si, the optical properties of a a:Si-H sample strongly depend on the fabrication process, which impacts the extend of disorder in the amorphous structure and the extend of weak bonds presence, explaining why stable a-Si:H waveguides have also been reported under similar illumination conditions [35]. Moreover, in [5], it has been pointed out that the degradation rate highly depends on the propagation conditions. Wide waveguides (800 nm-wide) might not show any degradation under illumination while smaller (500 nm-wide) waveguides on the same chip degrade significantly after only a few minutes, with picosecond input pulses (see in Fig. 5). Interestingly, the spectra of the generated SC with shorter ($< 200$ fs) input pulses in the same 500 nm-wide waveguides show no evidence of any degradation. This is confirmed in the power transmission recorded under 2 hours of continuous illumination as seen in Fig. 5.

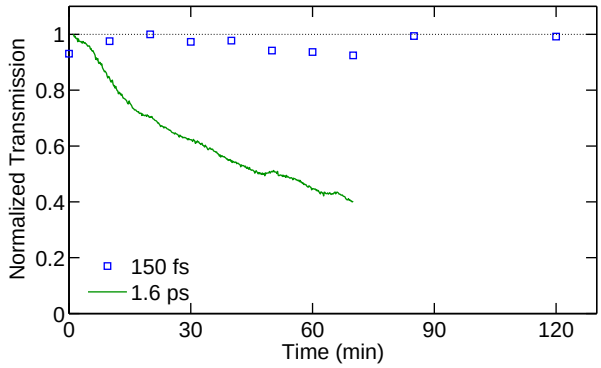


Fig. 5. Transmission, normalized to its maximum value, for 188 fs and 1.5 ps input pulse and similar peak power of about 12 W. The two measurements where taken with the same post-annealed waveguide.

## 7. SC generation in a:Si-H and c-Si waveguides

Few years ago, it has been realized that amorphous silicon shows better performance regarding instantaneous third order nonlinearities at telecommunication wavelengths than its crystalline counterpart [16, 36, 37, 25]. Thanks to a larger energy bandgap around 1.6-1.7 eV, a-Si:H is characterized by a lower nonlinear absorption coefficient around 1550 nm while keeping a large instantaneous Kerr effect, giving rise to an overall higher nonlinear figure-of-merit (FOM). By exploiting this high FOM, key experiments such as wavelength conversion [17, 18, 38], parametric amplification[16], supercontinuum generation with picosecond pulses [5], or ultrafast all-optical modulation [39] or waveform sampling [40], have been conducted in a-Si:H structures, and demonstrate its potential for low power ultrafast silicon based photonic technologies.

In order to prove the advantage of a-Si:H over c-Si for supercontinuum generation with femtosecond pulses, we have made a direct comparison between SCG in both structures. The dispersion properties of c-Si waveguides, fabricated with the same mask as for a-Si:H, have been measured with the same setup as discussed in section 3. As can be seen in Fig. 2, the 500 nm-wide c-Si and a:Si-H waveguides show similar dispersion properties and both have their ZDW around 1700 nm. The free-carriers effects being negligible in the dynamics of SCG in our c-Si waveguides [8], the only fundamental differences between the two waveguides lie in the real and imaginary parts of the nonlinear parameter $\gamma$ in Eq. 1. Because of large TPA at telecommunication wavelengths, the SPM induced spectral broadening of the pump pulse is clearly lower for c-Si than for a-Si:H waveguides (see Fig. 6). For a 1575 nm pump, the dispersive wave wavelength in the normal GVD regime is too far from the pump wavelength for this energy transfer to occur in c-Si. On the contrary, in the a-Si:H photonic wire, the peaks around the DW wavelength at 1900 nm are well developed. As previously discussed, we can even expect these peaks to be higher in shorter a-Si:H waveguides. At a pump wavelength closer to the ZDW, the DW became visible in the spectrum at the output of the c-Si waveguide, while for the a-Si:H one, the SC is at least four times broader and fully connected. Given the recent results in c-Si waveguides for shorter pump pulses of 80 fs [9], based on numerical simulations, we can expect by pumping our a-Si:H waveguide at 1550 nm to easily generate an almost flat SC between the two dispersive waves around 1200 nm and 2000 nm.

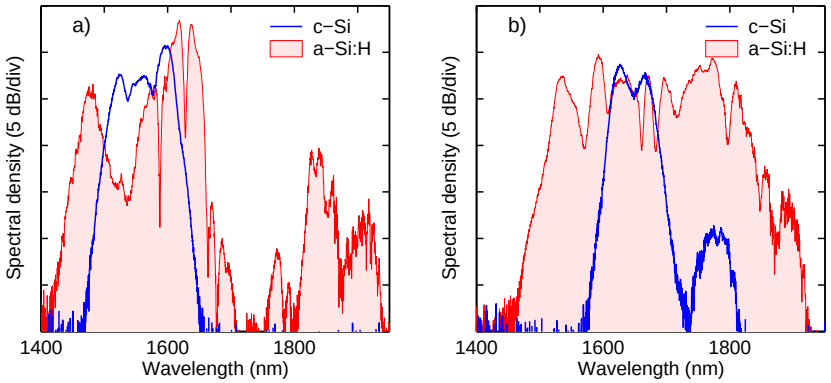


Fig. 6. Supercontinuum generation in similar waveguides made up of a-Si:H or c-Si. The dispersion curve of these waveguides are displayed in Fig. 1. The pump wavelength is $\lambda_s = 1575$ nm (a) and $\lambda_s = 1650$ nm (b).

## 8. Conclusions

We have experimentally studied the generation of supercontinuum in hydrogenated amorphous silicon photonic wires in the femtosecond regime at telecommunication wavelengths. Thanks to an engineered dispersion through the waveguide width, the waveguide dispersion is anomalous in the C-band. The numerical simulations based on the experimentally measured dispersion curve shows that the anomalous dispersion enable a strong temporal compression down to 15 fs starting from a 180 fs pump pulse. Following the compression, the pulse experiences high-order soliton fission as well as dispersive wave generation leading to a broad output spectrum spanning from 1420 nm to 1950 nm. The spectral broadening in a-Si:H photonic wire was demonstrated to be significantly larger than in crystalline waveguides with similar cross section and dispersion properties. The agreement between simulations and experiments shows that a simple model taking high-order dispersion, instantaneous refractive and absorptive nonlinear effects, and self-steepening is sufficient to capture the overall dynamics of the SC generation in our a-Si:H waveguide with femtosecond input pulses. We have demonstrated that the generated supercontinuum is highly coherent as expected from soliton fission dynamics [2]. Moreover, contrary to previous work in the picosecond regime, the a-Si:H waveguides have not shown any material degradation, nor in the SC spectrum nor in the power transmission.

a-Si:H waveguides thus appear as an interesting platform for applications requiring on chip coherent low power broad supercontinuum or ultrashort ($< 20$ fs) pulses at telecommunication wavelengths, where low-power pump pulse lasers in the range 100-200 fs are readily available. Moreover, thanks to low two-photon absorption, a-Si:H photonic wires are ideally suitable for the demonstration, in silicon-based technology, of new phenomena related to optical event horizon and/or dispersive waves [41, 42].

## Acknowledgment

This work was supported by the Belgian Science Policy Office (BELSPO) Interuniversity Attraction Pole (IAP) project Photonics@be and by the Fonds de la Recherche Fondamentale Collective, Grant No. 2.4563.12. Part of this work was carried out in the framework of the FP7-ERC projects MIRACLE and InSpectra. B. Kuyken acknowledges the special research fund of Ghent University (BOF), for a post doctoral fellowship.